SaSDim:Self-adaptive Noise Scaling Diffusion Model for Spatial Time Series Imputation

Shunyang Zhang, **Senzhang Wang**, **Xianzhen Tan**, **Renzhi Wang**
Ruochen Liu, **Jian Zhang** and **Jianxin Wang**
Central South University
{224712166, szwang, 224712155, rzwang, 234712122, jianzhang, jxwang}@csu.edu.cn,

Abstract

Spatial time series imputation is of great importance to various real-world applications. As the state-of-the-art generative models, diffusion models (e.g. CSDI) have outperformed statistical and autoregressive based models in time series imputation. However, diffusion models may introduce unstable noise owing to the inherent uncertainty in sampling, leading to the generated noise deviating from the intended Gaussian distribution. Consequently, the imputed data may deviate from the real data. To this end, we propose a **S**elf-**a**daptive noise **S**caling **Di**ffusion **M**odel named SaSDim for spatial time series imputation. Specifically, we introduce a novel Probabilistic High-Order SDE Solver Module to stabilize the noise following the standard Gaussian distribution. The noise scaling operation helps the noise prediction module of the diffusion model to more accurately estimate the variance of noise. To effectively learn the spatial and temporal features, a Spatial guided Global Convolution (SgGConv) module is also proposed. SgGConv effectively captures the multi-periodic temporal dependencies using Fast Fourier Transform (FFT), while also learning the dynamic spatial dependencies through dynamic graph convolution. Extensive experiments conducted on three real-world spatial time series datasets verify the effectiveness of SaSDim.

1 Introduction

Spatial time series is a type of data that describes the time series relationship within and between locations distributed across space, such as the traffic flow data collected from a set of road sensors deployed in a road network [Wang *et al.*, 2020]. To collect the observations of spatial time series, generally, a significant number of sensors, such as cameras and traffic sensors, are needed to be deployed. However, a complete spatial time series is usually unavailable due to various factors, including sensor malfunctions, unstable communication signals, non-uniform sensor distribution, and the stochastic and dynamic nature of data, leading to data anomalies or missing [Lim and Zohren, 2021]. Therefore, how to impute the incomplete spatial time series data is a primary challenge that needs to be addressed before further data analysis.

Traditionally, statistical methods such as ARIAM [Nelson, 1998] and HR [Xu *et al.*, 2022] are adopted for modeling time series. To further capture the spatial correlations of the time series data collected from different locations, matrix completion, and tensor decomposition approaches are utilized [Yu *et al.*, 2016]. However, it is difficult for these statistical based methods to capture the complex spatiotemporal relationships. Recently, deep learning methods such as CNN, RNN, and transformer have also been widely adopted for spatiotemporal data imputation. The RNN-based models, such as BRITS [Cao *et al.*, 2018] and ASTCMCN [Wang *et al.*, 2022a], impute missing values in an autoregressive way. However, biases can accumulate within the recursive structure of RNNs, ultimately impacting the model accuracy. CNN-based models try to capture the temporal correlations of the time series with convolutional kernels. However, the limited receptive field of CNN makes it difficult to capture global temporal correlations [Hewage *et al.*, 2020]. To address this issue, transformer-based models such as SAITS [Du *et al.*, 2023] and SPIN [Marisca *et al.*, 2022] apply attention mechanism to capture the global temporal dependencies. To model the multi-periodicity in time series, State Space Models (SSM) uses Fast Fourier Transform (FFT) to project time series from the time domain to the spectral domain, and aggregates features with different frequencies in the spectral domain [Gu *et al.*, 2021; Nguyen *et al.*, 2022]. However, SSM cannot effectively learn the spatial features of spatial time series.

Recently, diffusion models have been applied for spatial time series imputation and achieved better performance than autoregressive based methods. As the first diffusion model-based method, CSDI [Tashiro *et al.*, 2021] utilizes score-based diffusion conditioned on observed data for time series imputation. SSSD [Alcaraz and Strodthoff, 2022] further combines diffusion models and structured state space models to more effectively capture the long-term temporal dependencies in time series data. Generally, diffusion models create a forward process that learns a map from the ground truth to noise and a backward process to reconstruct data from noise to ground truth. Specifically, the forward process in diffusion models introduces the Gaussian noise into the data step by step. However, due to the uncertainty of sampling, the distribution of sampled noise may not really follow the Gaus-

sian distribution. This inconsistency may lead to bias, thus ultimately causing the imputed data to deviate from the real data. Another issue of current diffusion models is that they are less effective to capture the complex spatial and temporal features of the spatial time series data. For example, the multi-periodic temporal dependencies in time series are hard to be learned by CSDI and SSSD models.

To address the above issues, we propose a Self-adaptive Noise Scaling Diffusion Model named SaSDim. SaSDim can adaptively scale the sampled noise in the forward process to make the distribution of the noise more stable, and effectively capture the multi-periodicity temporal dependencies and dynamic spatial dependencies. Specifically, SaSDim contains three major modules, the Conditional Mixture Module, the **S**patial **g**uided **G**lobal **C**onvolution (SgGConv) module, and the Probabilistic High-Order Stochastic Differential Equation (SDE) Solver Module. The Conditional Mixture Module encodes the spatial time series data and extracts the multi-periodicity temporal features with FFT. Inspired by SGConv [Li *et al.*, 2022], SgGConv explicitly models the temporal dependencies with different time scales and captures the dynamic spatial dependencies. To be specific, SgGConv first decomposes a time series into components with different frequencies in the spectral domain. Then SgGConv measures the importance of each component by linearly combining each frequency and projects these frequencies back to the time domain to explicitly model the multi-periodic time series. The frequencies are further combined with the spatial convolution, which reflects spatial correlations among the time series generated from different locations. Finally, we use the Probabilistic High-Order SDE Solver Module to scale the noise at each time step by generating and optimizing the learnable coefficient of high-order SDEs. The primary contributions of this work are summarized as follows.

- We for the first time introduce a noise scaling mechanism in diffusion model to address the data generation bias issue caused by unstable noise sampling in forward process for more accurate spatial time series imputation.
- We propose the **S**patial **g**uided **G**lobal **Conv**olution module named SgGConv to effectively capture the complex spatial correlations as well as the multi-periodic temporal dependencies simultaneously.
- Extensively evaluations on three real-world datasets demonstrate that the proposed Probabilistic High-Order SDE Solver Module can effectively enhance the noise stability of the conventional diffusion models, and the SgGConv module can effectively capture the spatiotemporal correlations.

2 Related Work

Traditionally, statistical methods were used for time series imputation, such as K-Nearest Neighbors (KNN), Matrix Factorization (MF) [Yu *et al.*, 2016] and Multiple Imputation using Chained Equations. With the great success of deep learning models in spatial and temporal feature learning, RNN-based deep learning methods were also adopted. Deep autoregressive models based on recurrent neural networks (RNNs) are among the most popular approaches [Che *et al.*, 2018; Wang *et al.*, 2021; Yoon *et al.*, 2017]. BRITS [Cao *et al.*, 2018] is a representative model that utilizes bidirectional RNNs for spatial time series imputation and uses a linear regression layer to incorporate spatial information. Modeling the global temporal dependency is challenging for RNN models. To address this issue, SAITS introduced self-attention to capture the global temporal features [Du *et al.*, 2023]. SPIN further adopted joint attention that combined spatial and temporal attention to model information exchange between different time series [Marisca *et al.*, 2022]. ASTCMCN effectively combined transformer with RNN to capture both temporal and spatial dependencies for spatiotemporal data imputation [Wang *et al.*, 2022b].

Motivated by the great success of generative models, recent works tried to impute missing data using generative-based models. GAIN proposed to use generative adversarial networks (GANs) for data imputation [Yoon *et al.*, 2018]. GAINFilling tried to generate sequences by matching the underlying data distribution [Luo *et al.*, 2018]. CSDI proposed to apply Denoising Diffusion Probabilistic Models (DDPM) for data imputation [Tashiro *et al.*, 2021]. It sequentially employed feature and temporal attention to learn the noise at each step, while introducing conditions in the denoising process. However, these methods suffer from the issue of parameter explosion as the increase of the length of the time series, making researchers search for lightweight and more efficient feature extractors for time series modeling.

Recently, State Space Models (SSM) [**?**; Nguyen *et al.*, 2022; Goel *et al.*, 2022] have shown promising results in sequence modeling. SSM used a set of linear dynamics equations to model nonlinear and physical systems with input, output, and state variables. However, these models lack heuristics due to their long mathematical proof. Inspired by these methods, [Li *et al.*, 2022] proposed SGConv, which generated global convolution kernels by upsampling local convolution kernels before concatenating them. SGConv effectively modeled the distance-dependent decays among nodes in a sequence and kept the parameter scale sublinear with respect to the sequence length. While achieving promising results, SGConv cannot well catch the spatial information among graph nodes. This leads to limited performance improvement in time series imputation. More recently, a Fourier Transform-based deep method called TimesNet [Wu *et al.*, 2022] was proposed. It adapted the spectral characteristics of spatial time series to capture correlations within and across periods through multi-scale convolutions. However, limited by the convolutional kernel, TimesNet cannot effectively capture the spatial correlations and the multi-periodic temporal dependencies simultaneously.

3 Preliminary and Problem Definition

In this section, we will first define some terminologies, and then give a formal problem definition.

Definition 1. ***Spatial graph*** *Given the spatial distribution of the sensors (e.g. traffic sensors) for time series data collection, we construct a spatial graph* $G = (V, E)$ *based on the spatial distance between each pair of sensors, where*

Notations	Descriptions
$\boldsymbol{X}$	Spatial time series data
N	The number of the spatial nodes
$\beta_t, \alpha_t, \hat{\alpha}_t$	Constant hyperparameters of diffusion model
ϵ_θ	Noise prediction model
$\mathcal{F}$	Fast Fourier Transform
K	Convolutional kernel
G	Spatial graph
Δt	The cost of time from a time step to its neighbor step
∇	The first order derivative operator
r	The high order coefficient of SDE

Table 1: Important notations and corresponding descriptions.

$V = \{v_1, ..., v_N\}$ is a set of sensor nodes deployed in the space and E is the edge set connecting the sensor nodes.

Definition 2. ***Spatial Time Series.*** *We denote $X \in R^{N \times D}$ as the time series observations on spatial graph G. We denote the incomplete and complete spatial time series at time t as $X_t \in R^{N \times D}$and $Z_t \in R^{N \times D}$, respectively, where N is the number of spatial nodes (e.g. traffic sensors deployed at different locations) and D is the length of the time series.*

The historical spatial time series can be represented as a sequence $X = (X_{t-k}, ..., X_t)$. To conduct the spatial time series imputation over the locations where the data are unavailable, we also define the mask matrix of incomplete data as follows,

$$M_t(v_n) = \begin{cases} 0, & \text{if the corresponding value is missing} \\ 1, & \text{otherwise} \end{cases}$$

where v_n denotes the n-th sensor node and t is the time. $M_t(v_n)$ is a data mask matrix. We mark the element without observations as 0 and the element with data as 1.

To use the FFT, we need to introduce the convolution theorem first, which is a communication theory as follows,

$$\mathcal{F}(K * X) = \mathcal{F}(K) \cdot \mathcal{F}(X), \tag{1}$$

where $*$ is a convolution operation, $\cdot$ is a multiply operation. $\mathcal{F}$ represents FFT, which can be used to convolve time series. For time series X, it can be convolved by convolution kernel K by using FFT, which is similar to a time convolution operation.

Problem Definition 1. *Given the spatial graph $G = (V, E)$ and the corresponding incomplete spatial time series $X = (X_0, \ldots, X_T)$, we aim to build a model ϵ_θ to impute X and obtain a complete spatial time series $Z = (Z_0, \ldots, Z_T)$.*

4 Methodology

The model framework of SaSDim is shown in Figure 1, which contains the Conditional Mixture Module (CMM), the Spatial guided Global Convolution (SgGConv) module, and the Probabilistic High-Order SDE Solver Module (SDEM). CMM provides conditions to accelerate the convergence of SgGConv. SDEM aims to adaptively scale the predicted noise in the forward process. In summary, SaSDiM is a score-based conditional diffusion model. SgGConv and CMM integrate as the denoising score function, while SDEM outputs a high-order coefficient of the map from noisy data to the ground truth. Next, we will introduce the model in detail.

4.1 Conditional Mixture Module

In this module, we use a Conv1D encoder to embed the sequence relation and spatial information to guide the generation of a diffusion model. Specifically, the input data X_t in Figure 1 which contains noise during the denoising process, is first concatenated with a spatial time series data embedding that incorporates local information, which serves as a guidance for generation. Next, following the convolution theorem presented in the preliminary, the concatenated tensor is computed to extract the frequency feature through FFT. Then it is multiplied with convolution kernels from the SRGConv module and calculated from frequency feather to series. Additionally, diffusion embedding, feature embedding, and time step embedding are included as supplementary information and added to the tensor after this operation.

Then, the tensor goes through a layer of gated activation units before entering the next layer of residual units. The results of several residual layers are added to the output, which maintains its original state through skip connections, and then they are fed into the probabilistic high-order SDE solver. Briefly, we learn a function f in each residual layer. f transforms the input X_{L-1} to the output X_L.

$$X_L = f(X_{L-1}), \tag{2}$$

where L is the number of layers.

4.2 Spatial Guided Global Convolution Module

FFT is an effective tool to extract frequency features. In numerical computing, it is known as Discrete Fourier Transform (DFT) or FFT algorithm. DFT simplifies the numerous frequencies in a sequence to a smaller set of time series length L components. This helps us calculate their weighted sum, similar to the convolution operation.

Based on this idea and inspired by SGConv, we propose the spatial-guided Global Convolution. Convolutional kernels gather information from nearby neighbors in a sequence, following the "closer means stronger" rule [Li *et al.*, 2022]. For example, spatial graph convolution groups locations based on distances, and SGConv uses wave attenuation for temporal kernels. We further combine temporal kernels using graph spectrum information to build the spatial-guided global convolutional kernels. These represent a weighted sum of frequency components underlining each node, which can explicitly model the temporal correlations and dynamics.

Following this idea, we propose SRGConv which includes the Global Temporal Convolution and Dynamic Graph Convolution. First, the Global Temporal Convolution for modeling temporal correlation generates convolutional kernels K_i that build upon the wave curves with decay. Then we sum all the kernels as follows,

$$Sum(K) = \frac{1}{Z} \cdot \sum_{i=0}^{N_k} K_i, \tag{3}$$

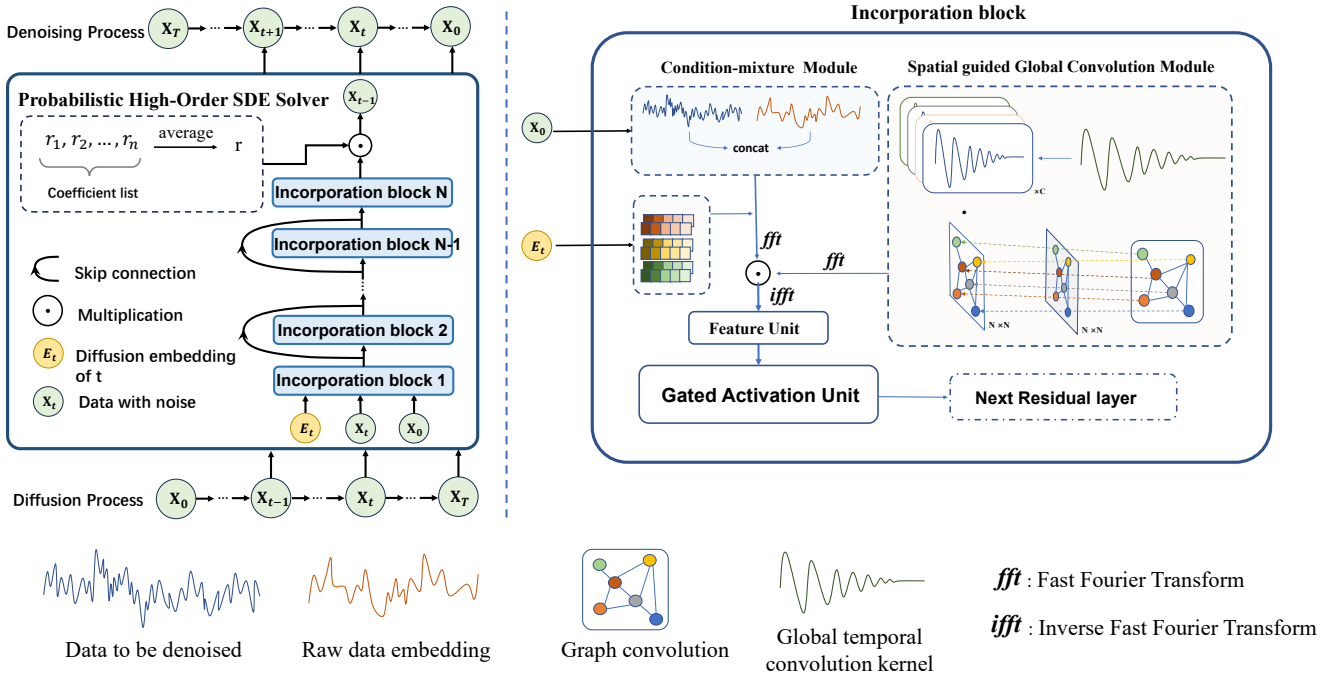

Figure 1: The model framework of SaSDim. The right side of the figure shows the details of the Conditional Mixture Module and the Spatial guided Global Convolution Module. The left side of the figure is the Probabilistic High-Order SDE Solver Module. The bottom is the explanation of symbols.

where N_k is the number of kernels. These kernels gather information from nearby elements in a time series. Following the DFT algorithm, it convolves temporal information by a weighted sum of the frequencies.

We next introduce the Dynamic Graph Convolution for modeling the spatial correlations. We have

$$A = f(W_\lambda(A)), \tag{4}$$

where W_λ is a scaling factor and f is the injection function which can be written as

$$W_\lambda = F(\alpha_0, \ldots, \alpha_N), \tag{5}$$

where $(\alpha_0, \ldots, \alpha_N)$ is the scaling factor corresponding to each node. The transformation F modifies the adjacent matrix among them with scaling factor so that we can inject it to the same size as time dimensions via injection function f. It is a dimensionality reduction so that the adjacent matrix can linearly combine the elements of the temporal kernel in the time dimension.

Finally, we combine the Global Temporal Convolution and Dynamic Graph Convolution by element-wise multiplication to obtain the Spatial guided Global Convolution. This combined operation $\varphi_{\bar{A}}(K)$ integrates the strengths of both convolutions, allowing for more comprehensive dynamic temporal information extraction, which can be written as

$$\varphi_{\bar{A}}(K) = \bar{A}K, \tag{6}$$

where $\bar{A}$ is calculated by $P\bar{\lambda_A}P^T$, P is a positive definite matrix and P^T is the transpose matrix of P with $\bar{\lambda_A}$ representing the eigenvalue matrix of A. According to the Convolution Theorem and Eq(6), the theorem equation can be rewritten as

$$F(\varphi_{\bar{A}}(K) * X) = F(\varphi_{\bar{A}}(K)) \cdot F(X). \tag{7}$$

Based on this formula, we compute a mapping from the time field to the spectral field and multiply them. Then we map the result back to the time field. During the process, frequency components are weighted and summed across nodes, where the kernel is regarded as the weight. Finally, we send the output from SgGConv to the Feature unit as shown in Figure 1, which can be considered as an attention to capture the spatial correlations.

4.3 Probabilistic High-Order SDE Solver

We first introduce the traditional stochastic differential equations (SDEs) that present the forward process. Then, we present our method that finds a new training loss to scale the unstable noise to a proper level. To be consistent with the representation of stochastic differential equations, $\boldsymbol{X}$ is denoted as x in the following sections.

First, SDEs perturb data to noise with a diffusion process governed by the following stochastic differential equation (SDE) [Yang *et al.*, 2022]

$$dx = f(x,t)dt + g(t)dw, \tag{8}$$

where $f(x,t)$ and $g(t)$ are diffusion and drift functions of the SDE, and w is a standard Wiener process. The forward process of denoising diffusion probabilistic model (DDPM)

discretizes the SDE so that it can be considered as the limit of the following discrete form as $\Delta t \to 0$:

$$x_{t+\Delta t} - x_t = f_t(x_t)\Delta t + g_t \Delta t \sqrt{\epsilon}, \quad (9)$$

$$\epsilon \sim N(0, I). \quad (10)$$

For the sampling process, given $t^{'} = t + \Delta t$, its discrete form can be written as follows,

$$\Delta x = -\left[f_t(x_t) - g_t^2 \nabla x_t \log q(x_t)\right] \Delta t + g_t \sqrt{\Delta t}\epsilon. \quad (11)$$

Continualizing this form, we can get

$$dx = [f(x,t) - g(t)^2 \nabla_x \log q_t(x)]dt + g(t)dw. \quad (12)$$

To achieve better results, we have computed the reverse process that includes higher-order derivatives.

Fact: The training loss function can be represented as:

$$\mathbb{E}_{Cond} \left\| \mathbf{s}_\theta(\mathbf{x_t}, \mathbf{t}) - (\mathbf{1} + \mathbf{r}) \nabla_{\mathbf{x_t}} \log \mathbf{q_t}(\mathbf{x_t}|\mathbf{x_0}) \right\|^2.$$

To prove that, we need two lemmas as follows,

Lemma 1. *High-order stochastic differential equation of equation (4) can be represented as*

$$dx = \psi(\nabla_x)dt + g(t)dw - \frac{1}{2} * \beta_x * g(t)^2 \nabla_{xx} \log q_t(x_t)dt,$$

when $\Delta t \to 0$ *and* $\psi(\nabla_x) = f(x,t) - g(t)^2 \nabla_x \log q_t(x)$. β_x *is an upper bound of* Δ_x.

Lemma 2. *Given the traditional sampling equations*

$$\Delta x = -\left[f_t(x_t) - g_t^2 \nabla x_t \log q(x_t)\right] \Delta t + g_t \sqrt{\Delta t}\epsilon,$$

we can get sampling equations of lemma1

$$\Delta x = -\left[f_t - (1+r) g_t^2 \nabla x_t \log q(x_t)\right] \Delta t + g_t \sqrt{\Delta t}\epsilon.$$

For more details of the two lemmas, one can refer to the Appendix.

By using stochastic differential equations to present the forward and backward process, we can calculate the score function $\Delta x_t \log p(x_t|x_0)$ (which can also be written as ϵ_θ or s_θ) which is equivalent to approximate ϵ. This is also called score matching [Song *et al.*, 2020]. Thus the coefficient of the score function can be written in Algorithm 1, line 7.

Regarding the range of r according to lemma2, we adopt a probabilistic sampling approach by sampling several points from a Gaussian distribution. Among these points, one is selected as the initial value for r. Considering that the magnitude of higher-order derivatives is smaller than that of the first-order derivative, the values of r are confined within a window on the Gaussian distribution.

During the training process, the noise predictor ϵ_θ is optimized to predict the noise each step with the help of the high order score function. Then we gain a high order coefficient r after each epoch optimizition. While selecting t in uniform distribution (Algorithm 1, line 3), its mathematical expectation is the average of all r. The mathematical expectation is varied according to the unstable noise. As a result, it scales down the intensity.

Algorithm 1 Training of SaSDiM

1: **Input:** Distribution of training data $q(x_0)$, the number of iteration N, the sequence of noise levels $\{\alpha_t\}$, high order coefficient r initialized as a variant;
2: **Output:** Trained denoising function ϵ_θ and a list of coefficient R;
3: **for** $i = 1$ **to** N **do**
4: $t \sim$ Uniform($\{1, \ldots, T\}$), $x_0 \sim q(x_0)$, R initialized as a list;
5: $\epsilon \sim \mathcal{N}(0, I)$;
6: Calculate noisy $x_t = \bar{\alpha}_t x_0 + \bar{\beta}_t \epsilon$;
7: Take gradient step on $\nabla_\theta ||(\epsilon - (1+r)\epsilon_\theta)||_2^2$, where $\epsilon_\theta = \epsilon_\theta(x_t, t \mid \hat{x_0})$;
8: $R[i] = r$;
9: **end for**

Algorithm 2 Imputation (Sampling) with SaSDiM

1: **Input:** Trained denoising function ϵ_θ, high order coefficient list R;
2: **Output:** Imputed missing values x_0;
3: $r = \sum_{i=1}^{N} R_i * (1/N)$;
4: $x_T \sim \mathcal{N}(0, I)$, where the dimension of x_T corresponds to the missing indices of $\hat{x_0}$;
5: **for** $t = T$ **to** 1 **do**
6: Sample x_{t-1} by using the sampling equations presented in **lemma2**;
7: **end for**

4.4 Implementation Details

The initialization of coefficient r of high-order SDE is in the range from 0 to 0.2. We set the maximum noise level to 0.02 and the layer of block to 4. The model is implemented using Pytorch and trained in an end-to-end manner using Adam with a learning rate of 0.001. We introduce the setting details in Table **??**.

5 Experiment

5.1 Datasets

We evaluate the performance of our model on three spatial time series datasets, METR-LA, AQI-36, and PEMS-BAY. METR-LA is a dataset used in traffic flow prediction and imputation. It contains 207 traffic sensor nodes in Los Angeles County Highway with a minute-level sampling rate. AQI-36 is collected from 36 AQI sensors distributed across the city of Beijing. This dataset serves as a widely recognized benchmark for imputation techniques and includes a mask used for evaluation that simulates the distribution of actual missing data [Yi *et al.*, 2016]. For a specific month, such as January, this mask replicates the patterns of missing values from the preceding month. Across all scenarios, the valid observations that have been masked out are employed as targets for evaluation. PEMS-BAY is an open dataset used for traffic flow prediction and analysis, primarily covering the transportation network of the Bay Area in California, USA. The dataset comprises 325 sensor nodes with a sampling interval of 5 minutes, and it contains a total of 16,937,700 data points.

Description	AQI-36	METR-LA	PEMS-BAY
Batch size	16	16	16
Time length L	24	24	24
Epochs	200	200	200
Learning rate	0.001	0.001	0.001
Channel size d	64	64	64
Minimum noise level β_1	0.0001	0.0001	0.0001
Maximum noise level β_T	0.5	0.2	0.2
Diffusion steps T	50	50	50

Table 2: The settings of SaSDiM for the three datasets.

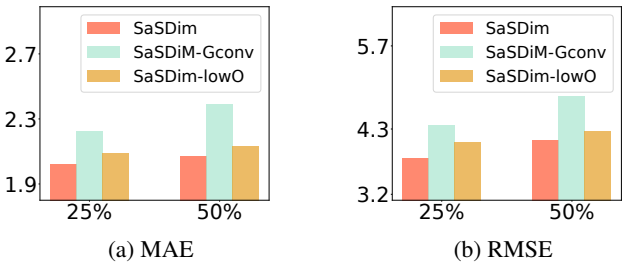

(a) MAE (b) RMSE

Figure 2: Performance comparison between SaSDiM and two variant models on the point data missing scenarios on METR-LA dataset.

In total, each dataset will be artificially masked 25% or 50% values at random. For the two datasets METR-LA and PEMSBAY, we partition the entire data into training, validation, and testing sets by a ratio of 8 : 1: 1. We evaluate our model performance under two metrics Mean Absolute Error (MAE) and Root Mean Square Error (RMSE).

5.2 Baselines

We compare our model with the following baselines.

- **Transformer** calculates the average value of nearby nodes based on geographic distance to impute.
- **SAITS** [Du *et al.*, 2023] is a method based on diagonally-masked self-attention (DMSA) and joint optimization.
- **BRITS** [Cao *et al.*, 2018] utilizes bidirectional RNN and MLP to integrate spatiotemporal features.
- **TimesNet** [Wu *et al.*, 2022] is a self-organized convolution model for time series imputation.
- **SPIN** [Marisca *et al.*, 2022] employs threshold graph attention and temporal attention jointly to implicitly model spatiotemporal sequences.
- **GRIN** [Cini *et al.*, 2022] is a bidirectional GRU-based method with graph neural network for multivariate time series imputation.
- **CSDI** [Tashiro *et al.*, 2021] is a probability imputation method based on the conditional diffusion probability model, which treats different nodes as multiple features of the time series, and uses a Transformer to capture the feature dependencies.

5.3 Experiment Result

The result shown in Table 3 indicates that BRITS performs not well among all the baseline models because the MLP model cannot effectively capture the spatial correlations and the higher-order relationships between nodes without a good spatial encoding. SAITS shows slightly better performance, indicating that Diagonally-Masked Self-Attention can alleviate the impact of self-redundant information and improve temporal prediction performance. SPIN outperforms other baseline models, suggesting that the improved attention mechanism with Hybrid Spatiotemporal Attention is effective in enhancing the performance of the original Transformer for spatial time series. The result of TimesNet results is slightly lower than those of SPIN from 1% to 10%, suggesting that while models that adaptively organize data for temporal convolution can effectively capture the temporal correlations, this convolution approach limits the ability to learn the global spatiotemporal dependencies. SaSDim achieves the best results in terms of two metrics in most cases with only three exceptions that achieve the second best results. Specifically, with a missing rate of 50% on the AQI-36 dataset, the MAE of SaSDim drops by 11% compared to SPIN. This confirms that the SgGConv module can better model the dynamic global temporal interaction. SaSDim achieves performance improvement by 7.5% compared to CSDI. One can also see that CSDI performs as well as SaSDim on the AQI-36 dataset but is surpassed by SaSDim by 20% on the METR-LA dataset. This demonstrates the superiority of SaSDim in modeling spatial time series compared with existing diffusion model-based approaches.

To further evaluate the performance of different methods under very high point data missing percentages, we compare SaSDiM against the baselines when $p\% = 75\%$ and $p\% = 95\%$. The result is shown in Table 4. It demonstrates again that SaSDiM outperforms all the baselines when the available time series observations are very sparse.

5.4 Ablation Study

To study whether each module of SaSDim is useful to the studied problem, we also compare SaSDim with two variants for ablation study. **SaSDim-lowO** is a variant of SaSDim that removes the probabilistic high-order SDE-solver module. **SaSDim-GConv** only captures the temporal global relations without using spatial guidance.

Figure 3 shows the RMSE and MAE bars for the two variants compared to SaSDim. It shows that SaSDim-GConv performs significantly worse than the other variants by 25% on 25% data missing scenario because it does not consider the geographical correlations between locations. The Constraint module is used to modulate the adjacency relationships between nodes.

SaSDim-lowO directly applies first-order derivatives in the denoising process. Although SaSDim-lowO is superior to other variants, it still performs worse than SaSDim, significantly lagging behind SaSDim with a 15% higher RMSE and

Model	AQI-36				PEMS-BAY				METR-LA			
	25%		50%		25%		50%		25%		50%	
	RMSE	MAE	RMSE	MAE	RMSE	MAE	RMSE	MAE	RMSE	MAE	RMSE	MAE
Transformer	29.46	16.26	31.49	17.45	2.98	1.63	3.22	1.74	7.01	2.82	7.16	2.89
BRITS	28.76	15.72	29.12	16.01	2.85	1.59	3.02	1.67	6.93	2.80	7.13	2.85
SAITS	29.85	16.24	30.97	17.18	2.34	1.35	2.57	1.42	6.23	2.66	6.51	2.73
CSDI	14.52	7.71	16.93	8.87	1.49	0.76	1.77	0.85	4.05	2.27	4.38	2.32
TimesNet	15.01	12.38	17.49	13.22	1.88	0.92	2.14	0.97	5.33	2.49	5.76	2.55
GRIN	12.93	7.93	15.81	9.02	1.70	0.85	1.92	0.91	4.21	2.30	4.47	2.35
SPIN	12.98	7.56	16.53	9.11	1.62	0.81	1.83	0.86	4.25	2.32	4.51	2.39
SaSDiM	**12.21**	**7.03**	**14.33**	**8.22**	**1.30**	**0.69**	**1.48**	**0.76**	**3.81**	**2.02**	**4.11**	**2.07**

Table 3: Comparison result between baselines and our method on AQI-36, METR-LA, and PEMS-BAY datasets. We report two error metrics RMSE and MAE for two missing percents in point missing.

Model	METR-LA		PEMS-BAY	
	75 %	95 %	75 %	95 %
BRITS	3.02	5.19	2.17	3.91
SAITS	3.74	6.72	2.96	7.40
Transformer	2.71	5.13	1.13	2.70
GRIN	2.39	4.08	1.09	2.70
SPIN	2.24	2.89	1.09	2.26
SaSDiM	**2.18**	**2.93**	**1.05**	**2.20**

Table 4: MAE comparison with increasing data sparsity in the *Point missing* setting.

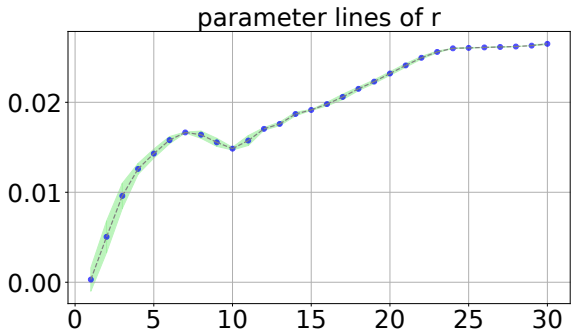

Figure 3: The orbit of coefficient r appeared in the loss function. The blue point is the median value of all batches at an epoch. The green area is the range of variance.

20% higher MAE in the 25% data missing scenario. This indicates that SaSDim can learn better representations by scaling down the noise for denoising.

5.5 Parameter Study

To analyze the parameter used in SaSDim, the scaling factor of the graph is initialized using a standard normal distribution. When the maximum value in the scaling factor array is larger than one, the values in the scaling factor array that are relatively smaller than the maximum value will become larger. Since the scaling factor array still follows a normal distribution, the difference between the maximum and minimum values will increase under equal probability. This led to an increase in the variance of the convolutional kernels and an increase in uncertainty. When the minimum value in the scaling factor array is smaller than zero, it greatly increases the uncertainty of the graph. For an extreme example, when all the coefficients in the scaling factor array are negative, the adjacency matrix becomes a negative matrix, causing the matrix to lose its physical meaning.

Finally, we study the effect of coefficients r of the probabilistic high-order SDE solver on the mode performance. According to the equation in the Appendix, the absolute value of r should be smaller than one, so we initially set the values of r to a value in the range between -1 and 1. To better observe the trajectory and trend of r during training, we set the initial value of r to zero. The results show that r gradually increases after a sudden decrease and eventually stabilizes around 0.026 as shown in Figure 3. This indicates that the noise scales down step by step. Next, to determine the final shared value of r for sampling, we conduct two experiments. In one experiment, we set r to be the last value obtained during optimization, and in the other experiment, we take the average of all the optimized r values. The results show that setting r to the last value obtained leads to significant fluctuations in performance while using the average value yields stable results. This suggests that taking the average value mitigates the impact of randomness.

6 Conclusion

This paper proposes a method called SaSDim inspired by global convolution and Denoising Diffusion Probabilistic Model learning framework for spatial time series imputation. SaSDim employs SgGConv to capture the global dynamic interactions among time steps. SgGConv models the temporal correlations with spatial information by generating dynamic temporal convolution kernels with spatial guidance. SaSDim optimizes the coefficients r of the high-order SDE solver during the training process to facilitate the generation of shared coefficients that scale unstable noise. Experimental results conducted on three real datasets verify the effectiveness of SaSDim.

A Provement

Lemma 1. High-order stochastic differential equation of equation(4) can be represented as

$$dx = \psi(\nabla_x)dt + g(t)dw - \frac{1}{2} * \beta_x * g(t)^2 \nabla_{xx} \log q_t(x_t)dt,$$

when $\Delta t \to 0$ and $\psi(\nabla_x) = f(x,t) - g(t)^2 \nabla_x \log q_t(x)$. And β_x is an upper bound of Δ_x.

Proof. Initially, the discretized form of a high-order stochastic equation can be written as

$$\begin{aligned} \Delta x = \psi(\nabla_x)\Delta_t + g(t)dw - \\ (\frac{1}{2!} * \Delta x * g(t)^2 \nabla_{xx} \log q_t(x_t) + \dots)\Delta_t. \end{aligned} \tag{13}$$

To go further, let's consider the third-order item as

$$\begin{aligned} \Delta x = \psi(\nabla_{xx})\Delta t + g(t)\Delta w - \\ (\frac{1}{3!}(\Delta x)^2 g(t)^2 \nabla_{xxx} \log q_t(x_t) + \dots)\Delta t. \end{aligned} \tag{14}$$

For the terms involving third-order derivatives, we have Δx raised to a higher power, and Δx is proportional to $\sqrt{t}$. Therefore, as Δt approaches zero, the third-order terms become higher-order infinitesimals with respect to Δt. By scaling, we can obtain

$$\begin{aligned} dx = [f(x,t) - g(t)^2 \nabla_x \log q_t(x)]dt + g(t)dw \\ -\frac{1}{2} * \beta_x * g(t)^2 \nabla_{xx} \log q_t(x_t)dt, \end{aligned} \tag{15}$$

where β_x is the upper bound of Δx. □

Based on lemma1, we prove

Lemma 2. Given the traditional sampling equations

$$\Delta x = -\left[f_t(x_t) - g_t^2 \nabla x_t \log q(x_t)\right] \Delta t + g_t \sqrt{\Delta t}\epsilon,$$

we can get sampling equations of lemma1

$$\Delta x = -\left[f_t - (1+r) g_t^2 \nabla x_t \log q(x_t)\right] \Delta t + g_t \sqrt{\Delta t}\epsilon.$$

Proof. Given that $q(x_t|x_0) = N(x_t; \bar{\alpha}_t x_0, {\bar{\beta}_t}^2 I)$, where $\bar{\beta}_t$ is the total noise intensity coefficient and we can get the equation below:

$$\nabla x_t \log q(x_t|x_0) = -\frac{x_t - \bar{\alpha}_t x_0}{{\bar{\beta}_t}^2} = -\frac{\bar{\epsilon}}{\bar{\beta}_t}. \tag{16}$$

Then the higher-order derivatives can be represented as

$$\nabla_{xx} \log q_t(x_t|x_0) * \Delta x_t = \alpha(\frac{\bar{\epsilon}}{\beta_{t+\Delta t}} - \frac{\bar{\epsilon}}{\beta_t}) = r_1 * \bar{\epsilon}, \tag{17}$$

as $\Delta x_t \sim O(\Delta(\sqrt{t}))$, α is limited to a finite real number. According to lemma1:

$$\begin{aligned} \Delta x = -\left[f_t(x_t) - g_t^2 \nabla x_t \log q(x_t)\right] \Delta t + \\ \beta_x * g(t)^2 \nabla_{xx} \log q_t(x_t)\Delta t + g_t \sqrt{\Delta t}\epsilon, \end{aligned} \tag{18}$$

and we get $\nabla x_t \log q(x_t)$ by

$$\begin{aligned} \nabla x_t \log q(x_t) &= \frac{\mathbb{E}_{x_0}[\nabla x_t q(x_t|x_0)]}{\mathbb{E}_{x_0}[q(x_t|x_0)]} \\ &= \frac{\mathbb{E}_{x_0}[q(x_t|x_0)\nabla x_t \log q(x_t|x_0)]}{\mathbb{E}_{x_0}[q(x_t|x_0)]}, \end{aligned} \tag{19}$$

then we get the result only by computing $q(x_t|x_0)$. Also, in the similar way we can compute $\nabla_{xx_t} \log q(x_t)$ with the rule of differentiation of fractions and the equation (8). Then we get it as

$$\nabla_{xx} \log q(x_t) = \frac{\mathbb{E}_{x_0}[q(x_t|x_0)\nabla_{xx} \log q(x_t|x_0)]}{\mathbb{E}_{x_0}[q(x_t|x_0)]}. \tag{20}$$

To go further, we have

$$\begin{aligned} \nabla x_t \log q(x_t) + \beta_x * \nabla_{xx} \log q_t(x_t) = \\ \frac{\mathbb{E}_{x_0}[q(x_t|x_0)(\nabla_x \log q(x_t|x_0) - \beta_x \nabla_{xx} \log q(x_t|x_0))]}{\mathbb{E}_{x_0}[q(x_t|x_0)]}. \end{aligned} \tag{21}$$

Finally, given $s_\theta(x_t, t) = \epsilon_\theta$, then the training loss can be presented as follows

$$\mathbb{E}_{Cond} \|\mathbf{s}_\theta(\mathbf{x_t}, \mathbf{t}) - (\mathbf{1}+\mathbf{r})\nabla_{\mathbf{x_t}} \log \mathbf{q_t}(\mathbf{x_t}|\mathbf{x_0})\|^2. \tag{22}$$

Given $t' = t + \Delta t$, then the sampling process can be written as:

$$\Delta x = -\left[f_t - (1+r) g_t^2 \nabla x_t \log q(x_t)\right] \Delta t + g_t \sqrt{\Delta t}\epsilon.$$

□

Acknowledgements

This research was funded by the National Science Foundation of China (No.62172443), the Science and Technology Major Project of Changsha (No.kh2402004) and Hunan Provincial Natural Science Foundation of China (No.2022JJ30053). This work was carried out in part using computing resources at the High-Performance Computing Center of Central South University.

Contribution Statement

Senzhang Wang is the corresponding author.

References

[Alcaraz and Strodthoff, 2022] Juan Miguel Lopez Alcaraz and Nils Strodthoff. Diffusion-based time series imputation and forecasting with structured state space models. *arXiv preprint arXiv:2208.09399*, 2022.

[Cao *et al.*, 2018] Wei Cao, Dong Wang, Jian Li, Hao Zhou, Lei Li, and Yitan Li. Brits: Bidirectional recurrent imputation for time series. *Advances in neural information processing systems*, 31, 2018.

[Che *et al.*, 2018] Zhengping Che, Sanjay Purushotham, Kyunghyun Cho, David Sontag, and Yan Liu. Recurrent neural networks for multivariate time series with missing values. *Scientific reports*, 8(1):6085, 2018.

[Cini *et al.*, 2022] Andrea Cini, Ivan Marisca, and Cesare Alippi. Filling the g_ap_s: Multivariate time series imputation by graph neural networks. In *ICLR*, 2022.

[Du *et al.*, 2023] Wenjie Du, David Côté, and Yan Liu. Saits: Self-attention-based imputation for time series. *Expert Systems with Applications*, 219:119619, 2023.

[Goel *et al.*, 2022] Karan Goel, Albert Gu, Chris Donahue, and Christopher Ré. It's raw! audio generation with state-space models. In *Proceedings of International Conference on Machine Learning*, pages 7616–7633. PMLR, 2022.

[Gu *et al.*, 2021] Albert Gu, Karan Goel, and Christopher Ré. Efficiently modeling long sequences with structured state spaces. *arXiv preprint arXiv:2111.00396*, 2021.

[Hewage *et al.*, 2020] Pradeep Hewage, Ardhendu Behera, Marcello Trovati, Ella Pereira, Morteza Ghahremani, Francesco Palmieri, and Yonghuai Liu. Temporal convolutional neural (tcn) network for an effective weather forecasting using time-series data from the local weather station. *Soft Computing*, 24:16453–16482, 2020.

[Li *et al.*, 2022] Yuhong Li, Tianle Cai, Yi Zhang, Deming Chen, and Debadeepta Dey. What makes convolutional models great on long sequence modeling? *arXiv preprint arXiv:2210.09298*, 2022.

[Lim and Zohren, 2021] Bryan Lim and Stefan Zohren. Time-series forecasting with deep learning: a survey. *Philosophical Transactions of the Royal Society A*, 379(2194):20200209, 2021.

[Luo *et al.*, 2018] Yonghong Luo, Xiangrui Cai, Ying Zhang, Jun Xu, et al. Multivariate time series imputation with generative adversarial networks. *Advances in neural information processing systems*, 31, 2018.

[Marisca *et al.*, 2022] Ivan Marisca, Andrea Cini, and Cesare Alippi. Learning to reconstruct missing data from spatiotemporal graphs with sparse observations. *Advances in Neural Information Processing Systems*, 35:32069–32082, 2022.

[Nelson, 1998] Brian K Nelson. Time series analysis using autoregressive integrated moving average (arima) models. *Academic emergency medicine*, 5(7):739–744, 1998.

[Nguyen *et al.*, 2022] Eric Nguyen, Karan Goel, Albert Gu, Gordon Downs, Preey Shah, Tri Dao, Stephen Baccus, and Christopher Ré. S4nd: Modeling images and videos as multidimensional signals with state spaces. *Advances in neural information processing systems*, 35:2846–2861, 2022.

[Song *et al.*, 2020] Yang Song, Jascha Sohl-Dickstein, Diederik P Kingma, Abhishek Kumar, Stefano Ermon, and Ben Poole. Score-based generative modeling through stochastic differential equations. *arXiv preprint arXiv:2011.13456*, 2020.

[Tashiro *et al.*, 2021] Yusuke Tashiro, Jiaming Song, Yang Song, and Stefano Ermon. Csdi: Conditional score-based diffusion models for probabilistic time series imputation. *Advances in Neural Information Processing Systems*, 34:24804–24816, 2021.

[Wang *et al.*, 2020] Senzhang Wang, Jiannong Cao, and S Yu Philip. Deep learning for spatio-temporal data mining: A survey. *IEEE transactions on knowledge and data engineering*, 34(8):3681–3700, 2020.

[Wang *et al.*, 2021] Qinfen Wang, Siyuan Ren, Yong Xia, and Longbing Cao. Bicmts: Bidirectional coupled multivariate learning of irregular time series with missing values. In *Proceedings of the 30th ACM International Conference on Information & Knowledge Management*, pages 3493–3497, 2021.

[Wang *et al.*, 2022a] Senzhang Wang, Jiyue Li, Hao Miao, Junbo Zhang, Junxing Zhu, and Jianxin Wang. Generative-free urban flow imputation. In *Proceedings of the 31st ACM International Conference on Information & Knowledge Management*, pages 2028–2037, 2022.

[Wang *et al.*, 2022b] Senzhang Wang, Jiyue Li, Hao Miao, Junbo Zhang, Junxing Zhu, and Jianxin Wang. Generative-free urban flow imputation. In *Proceedings of the 31st ACM International Conference on Information & Knowledge Management*, pages 2028–2037, 2022.

[Wu *et al.*, 2022] Haixu Wu, Tengge Hu, Yong Liu, Hang Zhou, Jianmin Wang, and Mingsheng Long. Timesnet: Temporal 2d-variation modeling for general time series analysis. In *The Eleventh International Conference on Learning Representations*, 2022.

[Xu *et al.*, 2022] Xin Xu, Liangliang Zhang, Qi Kong, Chenguang Gui, and Xing Zhang. Enhanced-historical average for long-term prediction. In *2022 2nd International Conference on Computer, Control and Robotics (ICCCR)*, pages 115–119. IEEE, 2022.

[Yang *et al.*, 2022] Ling Yang, Zhilong Zhang, Yang Song, Shenda Hong, Runsheng Xu, Yue Zhao, Yingxia Shao, Wentao Zhang, Bin Cui, and Ming-Hsuan Yang. Diffusion models: A comprehensive survey of methods and applications. *arXiv preprint arXiv:2209.00796*, 2022.

[Yi *et al.*, 2016] Xiuwen Yi, Yu Zheng, Junbo Zhang, and Tianrui Li. St-mvl: filling missing values in geo-sensory time series data. In *Proceedings of the 25th International Joint Conference on Artificial Intelligence*, 2016.

[Yoon *et al.*, 2017] Jinsung Yoon, William R Zame, and Mihaela van der Schaar. Multi-directional recurrent neural networks: A novel method for estimating missing data. In *Proceedings of Time series workshop in international conference on machine learning*, 2017.

[Yoon *et al.*, 2018] Jinsung Yoon, James Jordon, and Mihaela Schaar. Gain: Missing data imputation using generative adversarial nets. In *Proceedings of International conference on machine learning*, pages 5689–5698. PMLR, 2018.

[Yu *et al.*, 2016] Hsiang-Fu Yu, Nikhil Rao, and Inderjit S Dhillon. Temporal regularized matrix factorization for high-dimensional time series prediction. *Advances in neural information processing systems*, 29, 2016.